Dramatic Stabilization of the Native State of Human Carbonic Anhydrase II by an Engineered Disulfide Bond†

Lars-Göran Mårtensson,*,‡ Martin Karlsson,‡ and Uno Carlsson

IFM-Department of Chemistry, Linköping University, SE-581 83 Linköping, Sweden

Received June 25, 2002; Revised Manuscript Received October 15, 2002

ABSTRACT: To find a disulfide pair that could stabilize the enzyme human carbonic anhydrase II (HCA II), we grafted the disulfide bridge from the related and unusually stable carbonic anhydrase form from *Neisseria gonorrhoeae* (NGCA) into the human enzyme. Thus, the two Cys residues at positions 23 and 203 were engineered into a pseudo-wild-type form of HCA II (C206S), giving the mutant C206S/A23C/L203C. The disulfide bond was not formed spontaneously. The native state of the reduced form of the mutant was markedly destabilized (2.9 kcal/mol) compared to that of HCA II. Formation of a disulfide bridge was achieved by treatment by oxidized glutathione. This led to a significant stabilization of the native conformation. Compared to HCA II the unfolding midpoint for the variant was increased from 0.9 to 1.7 M guanidine HCl, corresponding to a stabilization of 3.7 kcal/mol. This makes the human enzyme almost as stable as the model protein NGCA, for which the unfolding of the native state has a midpoint at 2.1 M guanidine HCl. The stabilized protein underwent, contrary to all other investigated variants of HCA II, an apparent two-state unfolding transition, as judged from intrinsic Trp fluorescence measurements. A molten−globule intermediate is nevertheless formed but is suppressed because of the high denaturant pressure it faces upon rupture of the native state.

A major goal of protein engineering is the design of stabilized protein variants, and several strategies have been employed to achieve this objective, for example, helix dipole stabilization (*1*, *2*) and the classical method entailing introduction of novel disulfide bridges (reviewed in ref *3*). However, considering the latter approach, most attempts that have been successful have dealt with T4 lysozyme (*4*, *5*) and ribonuclease H (*6*).

Human carbonic anhydrase II (HCA II) is mainly a β-sheet protein that has 10 β-strands that divide the structure into two halves (Figure 1A). The upper part of the molecule consists of an N-terminal domain as well as a major domain that comprises the active site and the lower part of a large hydrophobic core. HCA II has been widely used as a model system for analysis of the catalytic (*7*), protein folding (*8*, *9*), protein−chaperone (*10*), and protein−surface adsorption mechanisms (*11*).

In the present study, our objective was to introduce a disulfide bridge into HCA II as a means of stabilizing the enzyme. To assign the bridge to suitable positions, we took advantage of the recently described structure of the enzyme designated NGCA, a related carbonic anhydrase found in the bacterium *Neisseria gonorrhoeae* (*12*). Although the homology between HCA II and NGCA is not very high (sequence identity 38.5%) (*12*), the three-dimensional structure of the two enzymes is highly similar (Figure 1A). In

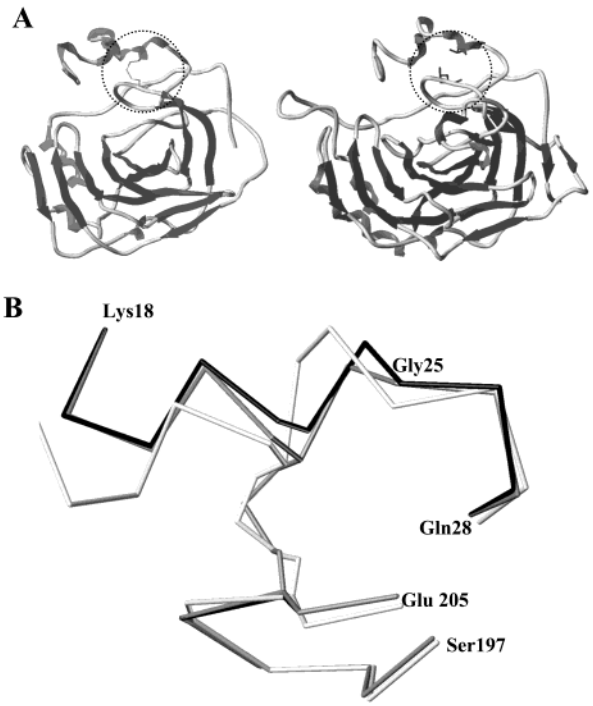

FIGURE 1: (A) Structures of NGCA and HCA II in which the disulfide bond and A23/L203, respectively, are encircled. (B) Superposition of the C_α trace in the vicinity of the disulfide bond in NGCA (white), the modeled, energy-minimized structure of HCA II with a disulfide bond between positions A23C and L203C (grey), and HCA II, before mutation and minimization (black). The numbering refers to HCA II.

† This work was supported by the Swedish Natural Science Research Council (U.C.), the Swedish Research Council (U.C., L.-G.M.), Stiftelsen Lars Hiertas Minne (L.-G.M., M.K.), and Magn. Bergvalls Stiftelse (L.-G.M.).

* To whom correspondence should be addressed E-mail: lgmar@ifm.liu.se. Fax: +46-13-281399. Phone: +46-13-285705.

‡ These authors contributed equally to this work.

[1] Abbreviations: A23C/L203C$_{red}$, reduced form of HCA II$_{pwt}$ with the mutations Ala23 → Cys and Leu203 → Cys; A23C/L203C$_{ox}$, oxidized form of HCA II$_{pwt}$ with the mutations Ala23 → Cys and Leu203 → Cys; ANS, 8-anilino-1-naphthalenesulfonic acid; DTT, dithiothreitol; GuHCl, guanidine hydrochloride; HCA II$_{pwt}$, pseudo-wild-type human carbonic anhydrase II, with a Cys206 → Ser mutation; IPTG, isopropyl-β-thiogalactopyranoside; NBD−Cl, 7-chloro-4-nitrobenzofurazan; NGCA, *Neisseria gonorrhoeae* carbonic anhydrase

10.1021/bi020433+ CCC: $22.00
Published on Web 12/04/2002

addition, NGCA has a disulfide bridge that corresponds to the buried residues Ala23 and Leu203 in HCA II, which makes this protein extremely stable (*13*) and therefore a suitable candidate model.

To fully describe the effects of the engineered disulfide bond on the stability of HCA II, we made three mutants, A23C, L203C, and A23C/L203C, and then used different methods to investigate the ability of these variants to withstand denaturation in guanidine-HCl (GuHCl). In summary, we report what is, to our knowledge, the first considerably stabilized variant of carbonic anhydrase. Moreover, we show that protein variants with desired properties can be designed by using evolutionarily related protein variants as a model.

MATERIAL AND METHODS

Materials. GuHCl, reagent-grade, was obtained from Pierce and was treated as described previously (*14*), and the concentration was determined by refractive index (*15*). 7-Chloro-4-nitrobenzofurazan (NBD−Cl) was obtained from Fluka, and 8-anilino-1-naphthalenesulfonic acid (ANS) was purchased from Sigma. All other chemicals were of reagent grade.

Site-Directed Mutagenesis, Protein Expression, and Protein Purification. To avoid unwanted disulfide formation, all mutations were made in pseudo-wild-type human carbonic anhydrase II ($HCAII_{pwt}$), containing the mutation C206S, as described earlier (*14*). The mutants were made using the site-directed mutagenesis kit Quik-Change purchased from Stratagene using the pACA vector (*14*, *16*), and mismatch oligonucleotides were purchased from DNA Technology A/S. After transformation a few colonies for each mutant were confirmed by DNA sequencing using Sangers dideoxy method (*17*).

The verified mutants were transformed into the expression strain BL21/DE3, and protein production was performed in 3 L of 2 × LB medium supplemented with 50 μg/mL of ampicillin. The cells were grown at 37 °C until an $OD_{600} \sim 0.8$. The temperature was lowered to room temperature, and the protein production was induced by addition of 0.50 mM IPTG (isopropyl-β-thiogalactopyranoside) and 0.50 mM zinc sulfate. The cells were grown overnight and harvested by centrifugation.

A suspension of the cells in 0.1 M Tris−H_2SO_4, pH 9.0, was lysed in an X-press (Biox), and after removal of cell debris by centrifugation of the supernatant, the enzymes were purified by affinity chromatography as described earlier (*18*). After purification the protein preparations were concentrated by ultra filtration (Amicon), using a membrane with a 10 kDa molecular weight cutoff. Further concentration (1−5 mg/mL) was performed using centrifugal filters, with a 10 kDa molecular weight cutoff (Millipore). The protein preparations were examined for purity and possible dimerization by SDS−PAGE.

Titration of Free Thiols. The content of free thiols was analyzed by labeling with 7-chloronitrobenzofurazan (NBD−Cl) after denaturation for 5 min in 5 M GuHCl before adding a 10-fold molar excess of the reagent. Quantification was done spectrophotometrically using an extinction coefficient of $\epsilon_{420\ nm} = 13\,000\ M^{-1}\ cm^{-1}$ for the NBD−sulfur adduct (*19*).

Disulfide Bond Formation. To initiate disulfide bond formation, the protein was first dialyzed against 0.01 M Tris−HCl, pH 8.5, overnight, and then 2 mM of oxidized glutathione was added to the enzyme solution (∼0.05−0.1 mM). Thereafter, glutathione and the oxidized protein were separated on a PD-10 column (Pharmacia). Possible dimers and aggregates were removed by size-exclusion chromatography on a Sephacryl S-200 column (dimensions, 90 × 1.8 cm; Pharmacia). The buffer used was 0.01 M Tris−HCl, pH 8.5 buffer, and the flow-rate was 1 mL/min.

Enzyme Activity Measurements. The esterase activity was measured using *p*-nitrophenyl acetate (pNPA) as a substrate, the absorbance change at 348 nm was registered, and the apparent second-order rate constant, k', was calculated according to Armstrong et al. (*20*).

CO_2 hydration activity was determined as described earlier (*21*, *22*).

CD Measurements. CD spectra were recorded in the near-UV region (240−320 nm) on a CD6 Spectrodichrograph (Jobin-Yvon Instruments), employing constant N_2 flushing. The protein spectra were corrected by a spectrum of a reference solution lacking the protein but otherwise identical to the sample. The ellipticity is reported as mean residue molar ellipticity ($[\theta]$, in deg·cm^2·dmol^{-1}) according to the equation

$$[\theta] = [\theta]_{obs} \cdot mrw/10lc$$

where $[\theta]_{obs}$ is the ellipticity (deg), mrw is the mean residue molecular weight (113.1 g·mol^{-1}), c is the protein concentration (g/mL), and l is the optical path length of the cell (cm). Near-UV spectra were obtained by scanning the proteins (17.1 μM) buffered with 10 mM Tris−H_2SO_4, pH 7, in a 5 mm quartz cell.

Stability Measurements. The stability of the HCAII variants was determined by various parameters (see below), after incubation of the enzyme (0.85 μM for the fluorescence and activity measurements and 8.5 μM for the CD measurements) overnight at 23 °C, in various concentrations of GuHCl containing 0.1 M Tris-H_2SO_4, pH 7.5. For the $A23C/L203C_{red}$ mutant, a 1000-fold (0.85 mM) molar excess of DTT was added to the incubation buffer.

Intrinsic Trp Fluorescence Measurements. Fluorescence spectra were recorded on each sample with the spectrofluorimeter (Hitachi F-4500) equipped with a thermostated cuvette holder. All spectra were recorded at 23 °C using a 1 cm quartz cuvette. The excitation wavelength was 295 nm, and three accumulative emission spectra were recorded in the wavelength region 310−400 nm, using 5 nm slits for both excitation and emission. From the spectra the wavelength of maximum emission was determined. The red shift of these spectra upon unfolding was then calculated.

CO_2 Hydration Measurements. Enzyme activity was determined by measuring the CO_2 hydration activity. Aliquots (30 μL) were withdrawn from the very same samples used for intrinsic Trp fluorescence measurements and transferred to the assay medium (3 mL veronal−H_2SO_4, pH 8.2). For the $A23C/L203C_{red}$ mutant, the assay medium was supplemented with a 1000-fold molar (0.85 mM) excess of DTT.

CD Measurements. The stability of $A23C/L203C_{ox}$ was also determined with CD in the near-UV region. CD spectra (240−320 nm) were registered using a 10 mm quartz cell

thermostated to 23 °C, and the value at 270 nm was plotted as a function of GuHCl concentration.

Data Analysis. The stability data were analyzed by a nonlinear least-squares fitting equation described by Santoro and Bolen (*23*), using the program TableCurve 2D (Jandel Scientific).

A linear dependence of the free energy transition was assumed in both transitions (*24*) according to the formula

$$\Delta G = \Delta G^{H_2O} - m[\text{GuHCl}] \quad (1)$$

The midpoint of denaturation, C_m, of each unfolding transition was determined from the ratio $\Delta G^{H_2O}/m$, when $\Delta G = 0$.

From the linear regression analysis of the data, the average correlation coefficients were found to be 0.98 for both tryptophan fluorescence measurements and activity measurements, respectively, and 0.98 for the single CD measurement.

The change in stability, $\Delta\Delta G$, was calculated as follows:

For the N → I transition,

$$\Delta\Delta G_{NI} = \Delta G_{NI}^{\text{Mutant}} - \Delta G_{NI}^{\text{Reference}} \quad (2)$$

The N → U transition was treated analogously.

ANS Binding. The binding of 8-anilino-1-naphthalenesulfonic acid (ANS) to protein in its molten−globule state, was examined by incubation of protein (8.5 μM) at various concentrations of GuHCl, 100 mM Tris−H_2SO_4 with a 20-fold excess of ANS present, overnight at 23 °C. Fluorescence emission spectra were recorded between 450 and 650 nm, and the intensity at emission maximum of the samples was plotted as a function of GuHCl concentration. The samples were excited at 360 nm, and excitation and emission bandwidths were 5 and 10 nm, respectively. The cuvette length was 1 cm, and the spectrofluorimeter was thermostated at 23 °C.

Computer Evaluation and Modeling. The coordinates from human carbonic anhydrase II (*25*) and carbonic anhydrase from *Neisseria gonorrhoeae* (*12*) were extracted from the Protein Data Bank operated by Research Collaboratory Structural Bioinformatics using the accession codes 2CBA and 1KOP, respectively. Structural details and computer modeling were performed on a Silicon Graphics workstation using the SYBYL 6.3 software (Tripos).

The structures of HCA II and NGCA was superimposed by matching the active-site histidines (His 94, 96, and 119 of HCA II and His 92, 94, and 111 of NGCA), giving an rms deviation of 0.19 Å between the matched histidines. The structures were visually inspected in order to determine which amino acids in the three-dimensional structure of HCA II that corresponds to the disulfide bridge between Cys28 and Cys181 in NGCA.

To create a possible model of an oxidized A23C/L203C mutant, a computer evaluation of the structure was performed. The Ala23 and Leu203 positions were mutated to cysteines and a disulfide bond was created between the two residues. To keep structurally conserved parts intact, only a subset of the structure (amino acids 19−27 and 203) was subjected to energy minimization while the rest of the molecule was treated as an aggregate. Essential hydrogens were added to the structure, and the energy minimization was performed using the Tripos force field, Kollman all-atom charges, a dielectric constant of 4 and a maximum of 5000 iterations, all other settings were default. The minimized structure was evaluated by comparing Ramachandran plots for the HCA II and the energy-minimized A23C/L203C structures.

Table 1: Properties of Mutation Sites in the HCA II Structure[a]

	properties			
protein	structural context	average *B*-factor[b]	fractional accessibility[c]	Δside chain volume[d] (Å^3)
C206S[e]	β-sheet	6.3	0.01	−13
A23C	3_{10} helix	10.7	0.08	+19
L203C	Turn	6.4	0.00	−38

[a] Data obtained from HCA II X-ray structure at 1.54 Å resolution (*25*). [b] The average *B*-factor for the backbone structure of the wild-type amino acid residue in each position. [c] Fractional accessibility was determined for the wild-type amino acid residue in each position. Fractional accessibility surface area was calculated as the ratio of the absolute area of each amino acid divided by the area of the exposed area of each amino acid situated in an exposed tripeptide, Ala-Xaa-Ala (*46*). Ratios larger than a value of 0.3, as a default value, were considered as exposed residues. [d] ΔSide chain volumes upon mutation were obtained using van der Waals volumes earlier calculated (*47*). [e] C206S is HCA II_{pwt}.

RESULTS

All the mutants in our study were constructed using a pseudo-wild-type template (HCA II_{pwt}) in which the single cysteine (Cys206) was mutated to a serine. This template was employed to avoid unwanted formation of disulfide bonds, and we have previously shown that it has properties that are indistinguishable from those of wild-type HCA II (*14*). Our objective of this study was to stabilize HCA II by introducing a disulfide bridge.

Design of the Mutants. Other isoenzymes of carbonic anhydrase, such as human CA IV (*26*) and CA VI (*27*), as well as the bacterial NGCA (*12*), contain Cys residues involved in a disulfide bond in positions that are structurally equivalent to the positions 23 and 203 in HCA II (*13*) (Figure 1). The presence of a disulfide bridge makes NGCA extremely resistant to denaturation in high concentrations of GuHCl. NGCA is very similar to HCA II in regard to three-dimensional structure (Figure 1A), showing an rms deviation of 1.35 Å between C^α atoms.

Examination of the HCA II structure (*25*) has revealed that both positions 23 and 203 are buried in the native state (Table 1), and the distance between the α-carbons is 6.3 Å, which is within the range of distances found between naturally occurring disulfides (*28*), indicating that, at this location, it would be possible to create such a bridge with reasonable angles and distances. Superposition and visual inspection of the two carbonic anhydrase structures also indicated that Ala23 and Leu203 of HCA II would be reasonable candidates for substitution to cysteines. Model building and simulation of a disulfide bond between positions 23 and 203 in HCA II resulted in a tentative model with an S−S torsional angle of 91.6°, an S−S bond length of 2.0 Å, and a C_α distance of 5.1 Å (Figure 1B). Gly25 was the monomer included in the energy minimization that underwent the largest conformational change with the ϕ angle moving from −69.0° to −84.4° and the ψ angle moving from 176.7° to −150.9°. Probably it is the conformational freedom

provided by the Gly25 (corresponding to Gly31 in NGCA), in the vicinity of A23C, that allows the disulfide bridge to be formed.

To carefully analyze the effects of the individual substitutions, we engineered three mutants: A23C, L203C, and A23C/L203C. The two amino acid residues that we replaced, A23 and L203, are situated in different structural contexts (i.e., in a 3_{10} helix and a turn, respectively), and the corresponding Cys mutations have opposite effects on the changes in side-chain volumes (Table 1). We used our standard protocol for culture and expression of the mutants (*29*), and the yield from a 1.5 L liquid culture varied from approximately 2.5 mg (L203C) to about 150 mg (A23C, A23C/L203C). All three mutants could be purified by affinity chromatography (*18*), indicating that they contained an intact active site.

SDS−PAGE and NBD−Cl titration were used to control the state of the three purified protein mutants at various stages. SDS−PAGE was run on all the mutants directly after purification, both with and without β-mercaptoethanol to analyze the purity and possible dimer formation during purification. For all the mutants, there were only one 30 kDa band on the gel, both under nonreducing and reducing conditions, indicating that the proteins were in a monomeric form. An NBD−Cl titration of the A23C/L203C mutant, under denaturing conditions, revealed that there was 2.0 mol free Cys per mol protein, meaning that no disulfide bridge was formed under these conditions in this variant, and only the reduced form of A23C/L203C was obtained after the purification procedure. To obtain the oxidized form of A23C/L203C, disulfide bond formation was induced by dialyzing the sample in 0.01 M Tris-H_2SO_4 (pH 8.5) and then adding oxidized glutathione, at room temperature. Size-exclusion chromatography was performed to remove excess reagent. After oxidation of the A23C/L203C, the SDS−PAGE gel revealed that some (∼20%) of the proteins had formed dimers. This fraction was subsequently separated from the monomeric form by size-exclusion chromatography, which was verified by SDS−PAGE. The amount of free thiols in the oxidized, monomeric form of A23C/L203C was determined by NBD−Cl titration under denaturing conditions and showed that no free Cys remained in the oxidized form (0.0 mol/mol protein). This demonstrates that the preparation was very homogeneous, containing only monomeric, oxidized A23C/L203C.

CD Spectra of the HCA II Variants. CD spectra in the near-UV range (240−320 nm) were recorded (Figure 2) to monitor the effect of the substitutions, and the spectral features of all the mutants were equivalent to those of a native carbonic anhydrase (*14*). However, for the L203C variant, the spectral bands showed only approximately 40% of the expected amplitude, probably due to partial denaturation as a result of the low stability of this mutant (Figure 3A).

Enzymatic Activity of the HCA II Variants. For all mutants both the CO_2 hydration activity and esterase activity were determined, and the results are summarized in Table 2. For all the mutants CO_2 hydration activity had decreased, and the activities of the reduced and the oxidized form of the A23C/L203C mutant were 85% and 55%, respectively, compared to the activity of HCA II_{pwt} (Table 2). However, the A23C mutation had no effect at all on the esterase activity. The L203C mutant exhibited low CO_2 hydration and esterase activity, but the decreased catalytic ability was likely due to instability of the mutant, as discussed above. The reduced and oxidized A23C/L203C variants showed 32% and 42% esterase activity, respectively.

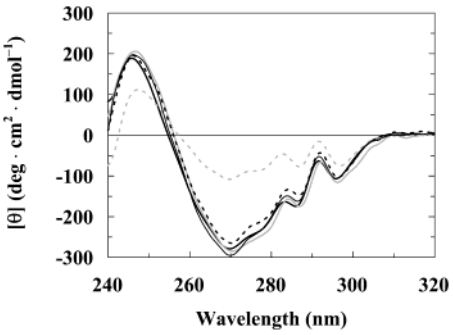

FIGURE 2: Near-UV CD spectra of the studied HCA II variants. HCA II_{pwt} (bold black line); A23C (gray line); L203C (gray dashed line); A23C/L203C_{red} (black dashed line); and A23C/L203C_{ox} (thin black line).

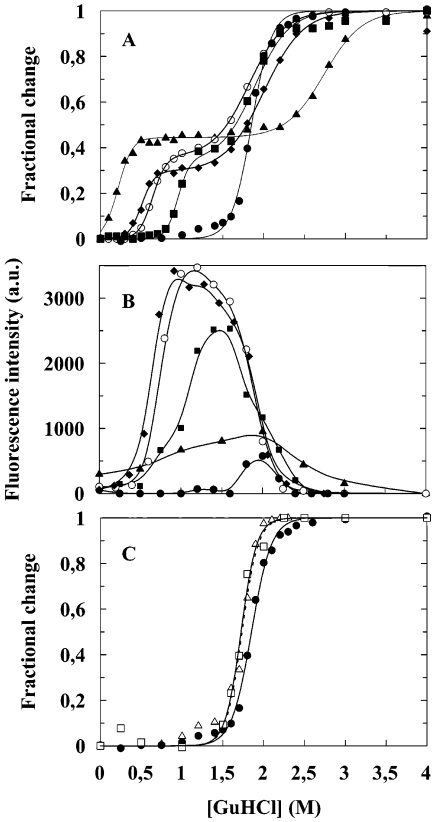

FIGURE 3: (A) Protein stability curves for HCA II variants, based on values obtained by Trp fluorescence measurements in various concentration of GuHCl. Symbols: (■) HCA II_{pwt}; (◆) A23C; (▲) L203C; (○) A23C/L203C_{red}; and (●) A23C/L203C_{ox}. All curves were fitted to a three-state transition (N → I → U), except that for the A23C/L203C_{ox} variant, which was fitted to a two-state transition (N → U). The parameters monitored are summarized in Table 3. (B) ANS binding displayed by the HCA II mutants in various concentration of GuHCl. Symbols: (■) HCA II_{pwt}; (◆) A23C; (▲) L203C; (○) A23C/L203C_{red}; and (●) A23C/L203C_{ox}. (C) Comparison of GuHCl denaturation curves for the A23C/L203C_{ox} variant, based on values obtained by monitoring: (△) CO_2 activity; (□) near-UV CD; and (●) Trp fluorescence.

Although the HCA II mutants displayed reduced enzyme activity compared to HCA II_{pwt}, they were still very active. This is indicated by the finding that, e.g., the 58% decrease

Table 2: Enzyme Activity for HCA II_{pwt}, Cys Mutants of HCA II_{pwt}, and NGCA as Monitored by CO_2 Hydration Activity and Esterase Activity

protein	enzyme activity[a]	
	CO_2 hydration (%)	esterase (%)
HCA II_{pwt}	100	100[b]
NGCA	79[c]	7[d]
A23C	50	100
L203C	10	18
A23C/L203C_{red}	85	32
A23C/L203C_{ox}	55	42

[a] Relative enzyme activities were calculated as percentage of HCA II_{pwt} enzyme activity. [b] The absolute value of HCA II_{pwt} was 1915 M^{-1} s^{-1}. [c] CO_2 hydration activity of NGCA was calculated as the ratio of k_{cat} from NGCA (*48*) and HCA II (*49*). [d] Esterase activity was calculated as the ratio of the NGCA value obtained from Chirica et al. (1997) (*48*) and the HCA II_{pwt} value.

in the esterase activity of the oxidized double mutant (A23C/L203C_{ox}) corresponded to an increase in activation energy of only 0.5 kcal/mol.

Stability Measurements. The global equilibrium unfolding behavior of the HCA II mutants can be analyzed by monitoring the wavelength shift of the intrinsic Trp fluorescence because HCA II has seven Trp residues distributed throughout the folded protein structure (*29*). The global unfolding of HCA II is a three-state process that proceeds via a stable molten−globule intermediate (N → I → U) (*14*); a similar three-state unfolding process has also been observed in HCA I (*30*). In our experiments, the midpoints of the first (N → I) and second (I → U) unfolding transitions of HCA II_{pwt} occurred at 1.0 and 1.9 M GuHCl, respectively. The unfolding of the A23C and L203C single mutants is also best described as a three-state process (Figure 3A; Table 3), in which, compared to HCA II_{pwt}, the first unfolding transition (N → I) occurs at lower GuHCl concentrations, with midpoints at 0.5 and 0.2 M GuHCl (A23C and L203C, respectively). Considering the second unfolding transition (I → U), the midpoint for the A23C mutant occurred at 2.0 M GuHCl, which is very similar to the corresponding value for HCA II_{pwt}, but was at the significantly higher concentration of 2.7 M GuHCl for the L203C mutant.

We measured the stability of both the reduced and the oxidized forms of the A23C/L203C double mutant (Figure 3A). The reduced form (A23C/L203C_{red}) exhibited an unfolding profile that was almost identical to that of the A23C single mutant, with midpoint unfolding at concentrations of 0.7 and 1.8 M GuHCl for the N → I and the I → U transition, respectively. However, the global unfolding reaction of A23C/L203C_{ox} appeared to be a two-state process, with the midpoint of unfolding at 1.8 M GuHCl (Table 3).

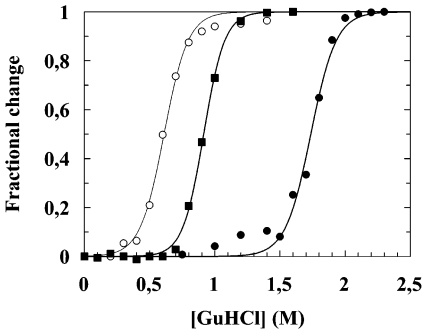

FIGURE 4: Protein stability curves based on CO_2 hydration activity measurements in various concentrations of GuHCl. Symbols: (■) HCA II_{pwt}; (○) A23C/L203C_{red}; and (●) A23C/L203C_{ox}.

To study unfolding of especially A23C/L203C_{ox} in greater detail, we examined three other parameters that could provide more specific structural information: ANS binding, near-UV CD spectral change at 270 nm, and decrease of CO_2 hydration activity. The various transitions monitored by these parameters were plotted as a function of GuHCl concentration (Figure 3B,C). We employed the hydrophobic fluorescent dye ANS to probe the formation of a molten−globule intermediate during the unfolding process; binding of ANS to a molten globule increases the intensity of fluorescence (*31*, *32*). For HCA II_{pwt}, there was a significant increase in the emission intensity accompanying the first global unfolding transition (N → I), with a maximum at 1.7 M GuHCl. A similar increase in emission intensity, accompanying to the N → I transition, was also observed for the A23C and A23C/L203C_{red} mutants. For the L203C mutant, the emission intensity was significantly lower, and no distinct peak was observed, probably due to partial denaturation of the enzyme also in the absence of GuHCl. The high stability of the molten globule of L203C is also supported by these ANS data. When ANS was added to A23C/L203C_{ox}, the rise in fluorescence intensity upon unfolding was much smaller, approximately 10% of that of HCA II_{pwt}, with a maximum at approximately 2.0 M GuHCl (Figure 3B). When we recorded denaturation as the change in near-UV CD ellipticity and enzyme activity (Figure 3C), the unfolding of A23C/L203C_{ox} appeared to be a two-state process. Moreover, these two unfolding curves coincided, but the midpoint of unfolding occurred at a somewhat lower concentration of GuHCl (1.7 M) than that indicated by the intrinsic Trp fluorescence measurements (1.8 M).

To estimate the extent to which the engineered disulfide bond increased the stability of the native state, we used the inactivation-unfolding curves of HCA II_{pwt}, A23C/L203C_{ox}, and A23C/L203C_{red} to calculate the stability in water (Figure 4). This was done because the enzyme activity reflects the

Table 3: Stability and Thermodynamic Parameters for GuHCl-Induced Unfolding for HCA II_{pwt} and Cys Mutants as Monitored by Trp Fluorescence Measurements[a]

protein	$C_{m_{NI}}$[b]	$\Delta G_{NI}^{H_2O}$	m_{NI}	$C_{m_{IU}}$[b]	$\Delta G_{IU}^{H_2O}$	m_{IU}	$C_{m_{NU}}$[b]	$\Delta G_{NU}^{H_2O}$	m_{NU}
HCA II_{pwt}	1.0	7.3	7.6	1.9	8.4	4.3			
A23C	0.5	3.9	7.7	2.0	5.2	2.6			
L203C	0.2	1.7	7.8	2.7	7.9	2.9			
A23C/L203C_{red}	0.7	4.5	6.9	1.8	5.4	3.0			
A23C/L203C_{ox}							1.8	11.0	6.0

[a] Units are as follows: ΔG, kcal mol^{-1}; m, kcal mol^{-1} M^{-1}; $C_{m_{NI}}$, M. [b] $C_{m_{NI}}$, $C_{m_{IU}}$, and $C_{m_{NU}}$ represent the transition midpoint concentration for the transition from the native (N) to the intermediate state (I), from the intermediate (I) to the unfolded state (U), and from the native (N) to the unfolded state (U), respectively.

Table 4: Stability and Thermodynamic Parameters for GuHCl-Induced Unfolding for HCA II_{pwt} and Cys Mutants as Monitored by CO_2 Hydration Activity Measurements[a]

protein	C_m[b]	ΔG^{H_2O}	m	$\Delta\Delta G^{H_2O}$
HCA II_{pwt}	0.9	7.1	7.6	
A23C/L203C$_{red}$	0.6	4.2	6.8	−2.9
A23C/L203C$_{ox}$	1.7	10.8	6.2	3.7

[a] Units are as follows: ΔG, kcal mol^{-1}; m, kcal mol^{-1}M^{-1} and C_m, M. [b] C_m represents the transition midpoint concentration obtained from the inactivation curve. The stability data were fitted to a two-state model as described in Material and Methods.

intactness of the active site and the native state of the molecule. The results given in Table 4 show that the stability of the native state of A23C/L203C$_{ox}$ was increased by 3.7 kcal/mol compared to HCA II_{pwt}. For comparison, we also used the Trp fluorescence unfolding curves to estimate the stability of the native state, and in this case, we included the single-point HCA II_{pwt} mutants (Table 3). The stability values obtained for the native conformation of A23C/L203C$_{ox}$ and A23C/L203C$_{red}$ were similar to those obtained from the enzyme activity measurements, and the native states of the single mutants A23C and L203C were found to be markedly destabilized (3.4 and 5.6 kcal/mol, respectively). For sake of completeness, we have also included the stability values of the molten globule ($\Delta G_{IU}^{H_2O}$) in Table 3, although these values are somewhat uncertain because of the long extrapolations to zero molar denaturant (*33*).

DISCUSSION

Special conformational criteria must be fulfilled to allow introduction of a novel disulfide bridge (e.g., ref *3*). Inability to satisfy these requirements often leads to strain in the folded structure, which in turn destabilizes the protein.

Fierke and co-workers (*34*) recently used an algorithm to find potential pairs for disulfide engineering in HCA II. From their results, it could be concluded that the algorithm was a good predictor of conceivable positions for disulfide bond formation between engineered Cys residues, but their experiments also revealed that additional factors must be included to identify stabilizing disulfide bonds. One of the selected disulfide pairs (L60C/S173C) was predicted to be highly favorable. However, it was found that the thermodynamic stability of a mutant with an engineered bond at that location was only marginally affected, as compared to the stability of wild-type HCA II. More specifically, the midpoint concentration of unfolding from the native to the molten−globule state (N → I) increased from 0.96 M for the wild-type enzyme to 1.02 M GuHCl for the mutant form.

To find a potential disulfide pair that could stabilize HCA II, we grafted the disulfide bridge from the related *Neisseria gonorrhoeae* carbonic anhydrase (NGCA) into the human enzyme; that is, we inserted two Cys residues at positions 23 and 203 in HCA II (see the results section). The presence of this disulfide bond makes NGCA remarkably stable, and its native state had an unfolding midpoint at 2.1 M GuHCl (*13*), as compared to 0.94 M for HCA II (*22*).

Effect of the Single-Substitution Mutations. The mutagenesis site at position 23 is located in a 3_{10} helix, and earlier mutagenesis and folding studies that were focused on this N-terminal region (*35*) have indicated that it functions as a "subdomain". It is noteworthy that the single substitution A23C led to a comparable destabilization of the native state of the protein (Table 3) that did a set of truncating mutations in this region (with the first 6−24 residues eliminated; *35*). On the other hand, the A23C substitution had no effect at all on the enzyme activity (Table 2). The changes in hydrophobicity and side-chain volume (Table 1) induced by replacement of an Ala with a Cys in a buried position is likely the cause of the destabilization of the native state of this mutant.

The other mutation site, position 203, is situated in the Thr199 loop (Ser197−Cys206), which is a part of the hydrophobic wall of the active site and contains Thr199, a residue that is important for the catalytic mechanism of the enzyme (*7*). The Thr199 loop forms a type VI turn (*36*) in which *cis*-Pro 202 plays a crucial role (*37*). This *cis*-Pro202 has been subjected to mutagenesis studies, and the crystallographic structure of a P202A mutant revealed that the cis configuration is retained in this variant (*38*). Obviously, Leu203 is located in a region that is structurally very restricted and rigid. We also noted considerable destabilization of the native conformation of the L203C mutant (5.6 kcal/mol), with an unfolding midpoint at 0.2 M GuHCl for the N→I transition (Table 3, Figure 3A). The enzyme activity of the L203C variant was only 18% of that exhibited by HCA II_{pwt} (Table 2). However, the CD spectrum of this mutant indicates that approximately 60% of the enzyme was denatured due to the low stability of the protein (Figure 2), which is also supported by the low yield of active enzyme (approximately 2.5 mg protein from 1.5 L of growth medium) and decreased specific activity after prolonged storage (weeks). Accordingly, we presumably underestimated the specific enzyme activity, which was probably of the same magnitude as that of the other mutants containing a Cys residue in position 203 (A23C/L203C$_{red}$ and A23C/L203C$_{ox}$; Table 2). Nevertheless, the activity was diminished in these mutants, and this is likely due to minor conformational changes of the catalytically essential Thr199 loop.

The A23C mutation did not have a significant impact on the second unfolding transition (I → U), a change responsible for disruption of the molten−globule intermediate (Figure 3A), which demonstrates that the stability of the molten globule was not affected by the substitution. This agrees with a large number of the mutations that we have previously performed (*8*, *39*). Thus, it appears that the native state of HCA II is more sensitive to mutations than the molten−globule intermediate, most likely due to the involvement of the side chains in specific tertiary interactions in the native state, which are essentially lacking in the molten globule. Moreover, it should be easier for the less compact and more flexible structure of the molten globule to accommodate larger side chains. In this context it is remarkable that the L203C mutation caused substantial stabilization of the molten−globule state (C_m = 2.7 M GuHCl), an effect that is difficult to explain but that was offset by the A23C mutation in both the oxidized and reduced double mutant (A23C/L203C; Figure 3A).

Effect of the Double-Substitution Mutations. Reduced A23C/L203C. Spontaneous formation of the disulfide bond did not occur in the double mutant A23C/L203C, which existed completely in reduced form upon purification. The native state of A23C/L203C$_{red}$ was significantly destabilized (2.8 kcal/mol) compared to HCA II_{pwt}. To ascertain whether

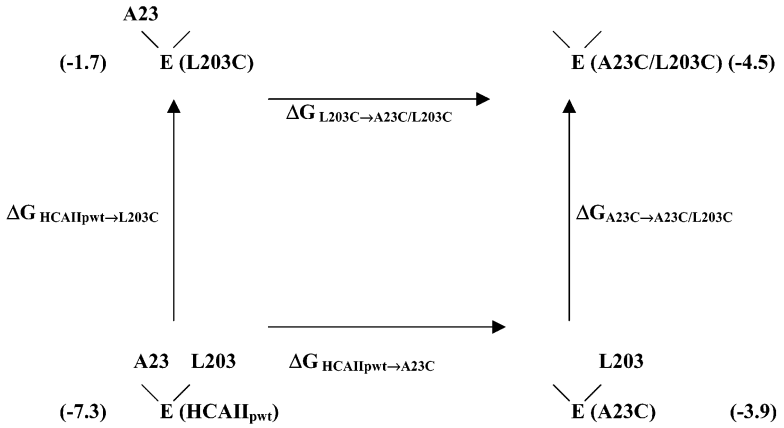

FIGURE 5: A thermodynamic double-mutant cycle for determining the coupling energy between Ala23 and Leu203 in the native state. The stability of the native state of each mutant is given within parentheses; these values were determined from the free energies of unfolding of the native state (Table 3). A23C/L203C is the reduced double mutant form.

there is interaction between the two residues in positions 23 and 203 in HCA II, we constructed a double-mutant cycle (*40*; Figure 5), using values from Trp-fluorescence measurements (Table 3). The coupling energy between Ala23 and Leu203 can be estimated by subtracting a value representing the change in free energy from L203C to A23C/L203C$_{red}$ ($\Delta G_{L203C\rightarrow A23C/L203C}$) from the value for the free energy change from HCA II$_{pwt}$ to A23C ($\Delta G_{HCAIIpwt\rightarrow A23C}$). Since the difference above is not null (−6.2 kcal/mol) there is a coupling between these two sites, indicating that the mutations in positions 23 and 203 are not independent.

Oxidized A23C/L203C. Formation of a disulfide bond did occur between the two inserted Cys residues in the double mutant A23C/L203C upon oxidation by oxidized glutathione. An interesting observation regarding A23C/L203C$_{red}$ is that there was a tendency toward oxidation of the Cys residues upon exposure to moderate concentrations of GuHCl. Using the CO_2 hydration activity assay to measure the ability of completely reduced A23C/L203C to withstand denaturation by GuHCl, we observed residual activity (∼40%) when the first unfolding transition was passed ($C_{m,NI}$ = 0.6 M GuHCl), and this lasted up to 1.7 M GuHCl (data not shown), a concentration at which the oxidized form of A23C/L203C is known to be inactivated. An NBD−Cl titration control of a reduced sample incubated in 0.8 M GuHCl verified that the active fraction of the enzyme had become oxidized under these conditions. Presumably, the presence of the denaturing agent made the structure surrounding Cys23 and Cys203 more flexible and thereby facilitated the rearrangements necessary for formation of the disulfide bond. After this observation the reducing agent DTT was included to prevent disulfide formation in both the GuHCl and activity assay solutions when analyzing the stability of A23C/L203C$_{red}$.

Introduction of the Cys23-Cys203 disulfide bond led to marked stabilization of the native conformation. Compared to HCA II$_{pwt}$, the unfolding midpoint for the mutant was moved from 0.9 to 1.7 M GuHCl, corresponding to a stabilization of 3.7 kcal/mol. To our knowledge, this is the first engineered variant of carbonic anhydrase to exhibit structure that is substantially more stable than that of the wild-type enzyme. The actual stabilization caused by the disulfide bridge was even greater (6.6 kcal/mol), since A23C/L203C$_{red}$ was 2.9 kcal/mol less stable than HCA II$_{pwt}$.

Comparing this stabilization with the stability of NGCA, Elleby and co-workers (*13*) have reported that the enzyme activity of NGCA was lost in GuHCl, with a midpoint of inactivation at a concentration of 2.1 M. Thus, the native state of A23C/L203C$_{ox}$ withstands GuHCl denaturation almost as well as native NGCA. Accordingly, the structural explanation for the greater stability of the bacterial enzyme seems to be due almost solely to the presence of the disulfide bridge, an assumption that is also supported by the data of Elleby et al. (*13*), showing that addition of a reducing agent lowered the inactivation midpoint to 1.2 M GuHCl. They also observed a second unfolding transition for NGCA with a midpoint at 2.9 M GuHCl (detected by Trp absorbance measurements), which, in analogy with HCA II, most likely reflects the disruption of a molten−globule intermediate.

Existence of Folding Intermediates. Thus far, all variants of HCA II that have been examined in equilibrium denaturation studies (using GuHCl) have been found to have a stable folding intermediate of molten−globule type (*8*). However, when we studied the unfolding reaction of A23C/L203C$_{ox}$ by recording the change in intrinsic Trp fluorescence, we observed only a two-state unfolding transition (Figure 3A). This prompted us to examine the unfolding process by monitoring other parameters that, in contrast to the global parameter Trp fluorescence, could probe unfolding in a more specific manner. The loss of enzyme activity is a very sensitive parameter, and small structural changes in the active site can suffice to cause inactivation, whereas the disappearance of the CD band might sense more global structural rearrangements that are linked to mobilization of the Trp side chains. Initially, it can be pointed out that the transition curves we obtained by recording the various parameters did not coincide (Figure 3C), which is evidence that A23C/L203C$_{ox}$ also undergoes sequential unfolding. The first event in unfolding of A23C/L203C$_{ox}$ entailed inactivation that occurred concomitant to the change in the CD band at 270 nm (C_m = 1.7 M), which implies that, at this stage, the active-site region was conformationally rearranged, and there was a concurrent loss of the asymmetric tertiary structure surrounding the aromatic residues, especially the Trp residues (*41*, *42*). Inasmuch as the unfolding transition revealed by internal Trp fluorescence occurred at somewhat higher GuHCl concentrations (C_m = 1.8 M) than the corresponding inactivation and CD transitions, the latter

changes do not reflect a transition to the fully unfolded state for A23C/L203C$_{ox}$. Since increasing ANS fluorescence accompanied the first unfolding transition, it is evident that this stabilized mutant also formed a molten−globule intermediate.

During the second unfolding transition, the Trp emission maximum shifted from 337 to 354 nm, corresponding to the native and fully unfolded state, respectively, and this is in accordance with data on several previously studied HCA II variants (e.g., ref *43*). We also observed very similar red shifts when the other mutants passed the two unfolding transitions. Consequently, the A23C/L203C$_{ox}$ variant did undergo a transition to the unfolded state in this GuHCl concentration range. Since this second unfolding transition partly overlapped the first, the molten globule that arose must have ruptured before the first unfolding transition was completed. Therefore, the amount of molten globule accumulated was considerably less (approximately 5−10%) for this mutant than for HCA II$_{pwt}$ or the A23C/L203C$_{red}$ mutant (Figure 3B). The lower amount of molten globule observed for the L203C mutant can be explained by partial denaturation of the unstable protein from the beginning.

Both the CD and the fluorescence measurements probe changes that occur in the environment around the Trp residues during unfolding of the protein. Specifically, near-UV CD reports on alterations in asymmetric properties of the substructure around the Trp residues, whereas the emission maximum shifts of the Trp residues reflect changes in polarity. Therefore, it appears that when the A23C/L203C$_{ox}$ molten globule was formed during the first unfolding transition, the tertiary interactions, at least those involving the Trp residues, were lost, and the intact structure of the active site was ruptured. However, during the initial stages of this unfolding event, there was no change in the intrinsic Trp fluorescence, which suggests that the polarity in the vicinity of the Trp residues was not altered during formation of the molten globule, but merely a mobilization of the Trp residues occurred. This means that the fluctuations in proximity of the Trp residues in the molten globule do not allow water to penetrate deeply enough into the molten globule to have an impact on the fluorescence emission of the Trp residues. In other words, the molten globule seems to be as dry as the native state. Subsequently, at higher denaturant pressure, there is an influx of water, monitored as a red shift in the Trp fluorescence, in connection with the unfolding of the molten−globule.

Reports concerning the molten−globule state have fairly recently demonstrated that nonnative proteins are more structured and less hydrated than commonly believed (*44*, *45*). This is opposite to the current view that the molten−globule state is an expanded, hydrated form of the native state. Thus, the unfolding behavior of A23C/L203C$_{ox}$ supports the novel idea proposed by the cited investigators.

Further stabilization of the native state of HCA II, achieved using A23C/L203C$_{ox}$ as a template, might make it possible to completely avoid accumulation of the molten−globule state and convert the protein to two-state unfolding behavior. In a previous study (*39*), we found that HCA II forms aggregates in the molten−globule state, and this leads to reduced yields of active enzyme during refolding. Therefore, it might be possible to improve the refolding yield by suppressing the molten−globule intermediate.

ACKNOWLEDGMENT

We thank Prof. Sven Lindskog, Umeå University, for providing us with unpublished data on the stability of carbonic anhydrase from *Neisseria gonorrheae*.

REFERENCES

1. Nicholson, H., Becktel, W. J., and Matthews, B. W. (1988) *Nature 336*, 651−656
2. Nicholson, H., Anderson, D. E., Dao-pin, S., and Matthews, B. W. (1991) *Biochemistry 30*, 9816−9828.
3. Betz, S. F. (1993) *Protein Sci. 2*, 1551−1558.
4. Matsumura, M., Becktel, W. J., Levitt, M., and Matthews, B. W. (1989) *Proc. Natl. Acad. Sci. U.S.A.* 86, 6562−6566.
5. Jacobson, R. H., Matsumura, M., Faber, H. R., and Matthews, B. W. (1992) *Protein Sci. 1*, 46−57.
6. Kanaya, S., Katsuda, C., Kimura, S., Nakai, T., Kitakuni, E., Nakamura, H., Katayanagi, K., Morikawa, K., and Ikehara, M. (1991) *J. Biol. Chem. 266*, 6038−6044.
7. Lindskog, S. (1997) *Pharmacol. Ther. 74*, 1−20.
8. Carlsson, U., and Jonsson, B.-H. (2000) in *The carbonic anhydrases: New horizons* (Chegwidden, W. R., Carter, N. D., and Edwards, Y. H., Eds.) pp 241−259, Birkhäuser Verlag AG, Basel, Switzerland.
9. Hammarström, P., and Carlsson, U. (2000) *Biochem. Biophys. Res. Commun. 276*, 393−398.
10. Persson, M., Lindgren, M., Hammarström, P., Svensson, M., Jonsson, B.-H., and Carlsson, U. (1999) *Biochemistry 38*, 432−441.
11. Karlsson, M., Mårtensson, L.-G., Jonsson, B.-H., and Carlsson, U. (2000) *Langmuir 16*, 8470−8479.
12. Huang, S., Xue, Y., Sauer-Eriksson, E., Chirica, L., Lindskog, S. and Jonsson, B.-H. (1998) *J. Mol. Biol. 283*, 301−310.
13. Elleby, B., Chirica, L. C., Tu, C. K., Zeppezauer, M., and Lindskog S. (2001) *Eur. J. Biochem. 268*, 1613−1619.
14. Mårtensson, L.-G., Jonsson, B.-H., Freskgård, P.-O., Kihlgren, A., Svensson, M., and Carlsson, U. (1993) *Biochemistry 32*, 224−231.
15. Nozaki, Y. (1972) *Methods Enzymol. 26*, 43−50.
16. Nair, S. K., Calderone, T. L., Christianson, D. W., and Fierke, C. A. (1991) *J. Biol. Chem. 266*, 17320−17325.
17. Sanger, F., Nicklen, S., and Coulson, A. R. (1977) *Proc. Natl. Acad. Sci. U.S.A. 74*, 5457−5463.
18. Khalifah, R. G., Strader, D. J., Bryant, S. H., and Gibson, S. M. (1977) *Biochemistry 16*, 2241−2247.
19. Birkett, D. J., Dwek, R. A., Radda, G. K., Richards, R. E., and Salmon A. G. (1971) *Eur. J. Biochem. 20*, 494−508.
20. Armstrong, J. M., Myers, D. V., Verpoorte, J. A., and Edsall J. T. (1966) *J. Biol. Chem. 241*, 5137−5149.
21. Rickli, E. E., Ghazanfar, S. A. S., Gibbons, B. H., and Edsall, J. T. (1964) *J. Biol. Chem. 239*, 1065−1078.
22. Mårtensson, L.-G., Jonsson, B.-H., Andersson, M., Kihlgren, A., Bergenhem, N., and Carlsson, U. (1992) *Biochim. Biophys. Acta 1118*, 179−186.
23. Santoro, M. M., and Bolen, D. W. (1988) *Biochemistry 27*, 8063−8068.
24. Schellman, J. A. (1978) *Biopolymers 17*, 1305−1322.
25. Håkansson, K., Carlsson, K., Svensson, L. A., and Liljas, A. (1992) *J. Mol. Biol. 227*, 1192−1204.
26. Stams, T., Nair, S. K, Okuyama, T., Waheed, A., Sly, W. S., and Christianson, D. W. (1996) *Proc. Natl. Acad. Sci. U.S.A. 93*, 13589−13594.
27. Fernley, R. T, Wright, R. D., and Coghlan, J. P. (1988) *Biochemistry 27*, 2815−2820.
28. Thornton, J. M. (1981) *J. Mol. Biol. 151*, 261−287.
29. Mårtensson, L.-G., Jonasson, P., Freskgård, P.-O., Svensson, M., Carlsson, U., and Jonsson, B.-H. (1995) *Biochemistry 34*, 1011−1021.
30. Rodionova, N. A., Semisotnov, G. V., Kutyshenko, V. P., Uverskii, V. N., Bolotina, I. A., Bychkova, V. E., and Ptitsyn, O. B. (1989) *Mol. Biol. (Moscow) 23*, 683−692.
31. Semisotnov, G. V., Rodionova, N. A., Kutyshenko, V. P., Ebert, B., Blanck, J., and Ptitsyn, O. B. (1987) *FEBS Lett. 222*, 9−13.

32. Semisotnov, G. V., Rodionova, N. A., Razgukaev, O. I., Uversky, V. N., Gripas, A. F., and Gilmanshin, R. I. (1991) *Biopolymers 31*, 119−128.
33. Pace, C. N., Vanderburg, K. E. (1979) *Biochemistry 18*, 288−292.
34. Burton, R. E., Hunt, J. A., Fierke, C. A., and Oas, T. G. (2000) *Protein Sci. 9*, 776−785.
35. Aronsson, G., Mårtensson, L.-G., Carlsson, U., and Jonsson, B.-H. (1995) *Biochemistry 34*, 2153-2162.
36. Richardson, J. S. (1981) *Adv. Prot. Chem. 34*, 167−339.
37. Krebs, J. F., and Fierke, C. A. (1993) *J. Biol. Chem. 268*, 948−954.
38. Tweedy, N. B., Nair, S. K., Paterno, S. A., Fierke, C. A., and Christianson, D. W. (1993) *Biochemistry 32*, 10944−10949.
39. Hammarström, P., Persson, M., Freskgård, P.-O., Mårtensson, L.-G., Andersson, D., Jonsson, B.-H., and Carlsson, U. (1999) *J. Biol. Chem. 274*, 32899−32903.
40. Horovitz, A., and Fesht, A. (1990) *J. Mol. Biol. 214*, 613−617.
41. Freskgård, P.-O., Mårtensson, L.-G., Jonasson, P., Jonsson B.-H., and Carlsson, U. (1994) *Biochemistry 33*, 14281−14288.
42. Borén, K., and Carlsson, U. (1999) *Biochim. Biophys. Acta 1430*, 111−118.
43. Hammarström, P., Owenius, R., Mårtensson, L.-G., Carlsson, U., and Lindgren, M. (2001) *Biophys. J. 80*, 2867−2885.
44. Denisov, V. P., Jonsson, B.-H., and Halle, B. (1999) *Nat. Struct. Biol. 6*, 253−260.
45. Jonasson, P., Kjellsson, A., Sethson, I., and Jonsson, B.-H. (1999) *FEBS Lett. 445*, 361−365.
46. Lee, B., and Richards, F. M. (1971) *J. Mol. Biol. 55*, 379−400.
47. Richards, F. M. (1974) *J. Mol. Biol. 82*, 1−14.
48. Chirica, L. C., Elleby, B., Jonsson, B.-H., and Lindskog, S. (1997) *Eur. J. Biochem. 244*, 755−760.
49. Khalifah, R. G. (1971) *J. Biol. Chem.* 246, 2561−2573.

BI020433+